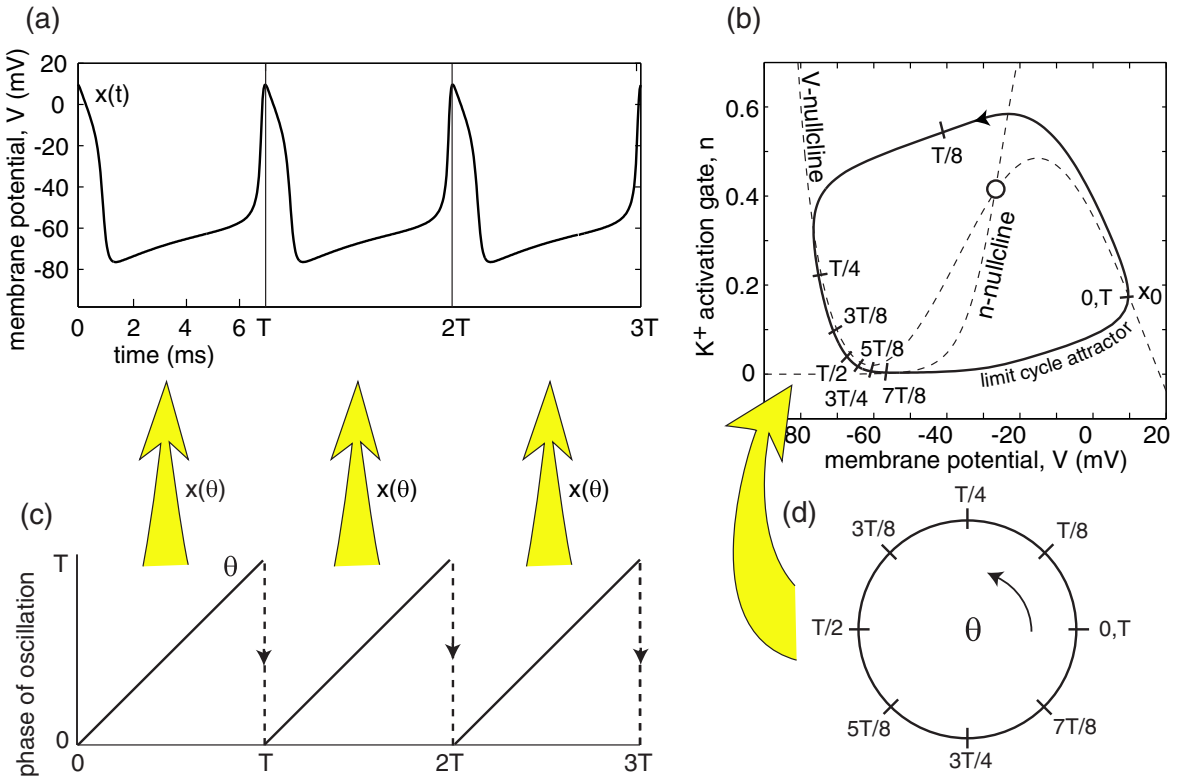

Figure 10.1: Definition of a phase of oscillation, ϑ, in the $I_{\rm Na} + I_{\rm K}$-model with parameters as in Fig.4.1a and $I = 10$.

oscillators.

10.1 Pulsed Coupling

In this section we consider oscillators of the form

$$\dot{x} = f(x) + A\delta(t - t_{\rm s}) \,, \qquad x \in \mathbb{R}^m, \tag{10.1}$$

having exponentially stable limit cycles and experiencing pulsed stimulation at times $t_{\rm s}$ that instantaneously increases the state variable by the constant A. The Dirac delta function $\delta(t)$ is a mathematical shorthand notation for resetting x by A. The strength of pulsed stimulation, A, is not assumed to be small. Most of the results of this section can also be applied to the case in which the action of the input pulse is not instantaneous, but smeared over an interval of time, typically shorter than the period of oscillation.

10.1.1 Phase of Oscillation

Many types of physical, chemical, and biological oscillators share an astonishing feature: they can be described by a single phase variable ϑ. In the context of tonic spiking, the

phase is usually taken to be the time since the last spike, as in Fig.10.1a.

We say that a function $x(t)$ is periodic if there is a constant $T > 0$ such that $x(t + T) = x(t)$ for any t. The minimal value of the constant is the period of $x(t)$. Periodic functions appear in dynamical systems having limit cycle attractors.

The notion of the phase of oscillation is related to the notion of parametrization of a limit cycle attractor, as in Fig.10.1b. Take a point x_0 on the attractor and plot the trajectory $x(t)$ with $x(0) = x_0$. Then the phase of $x(t)$ is $\vartheta = t$. As t increases past the period T, then $2T$, an so on, the phase variable ϑ wraps around the interval $[0, T]$, jumping from T to 0; see Fig.10.1c. Gluing together the points 0 and T, as in Fig.10.1d, we can treat the interval $[0, T]$ as a circle, denoted as $\mathbb{S}^1$, with circumference T. The parametrization is the mapping of $\mathbb{S}^1$ in Fig.10.1d into the phase space $\mathbb{R}^2$ in Fig.10.1b, given by $\vartheta \mapsto x(\vartheta)$.

We could put the initial point x_0 corresponding to the zero phase anywhere else on the limit cycle, and not necessarily at the peak of the spike. The choice of the initial point introduces an ambiguity in parameterizing the phase of oscillation. Different parametrizations, however, are equivalent up to a constant phase shift (i.e., translation in time). In the rest of the chapter, ϑ always denotes the phase of oscillation, the parameter T denotes the period of oscillation, and $\vartheta = 0$ corresponds to the peak of the spike unless stated otherwise. If the system has two or more coexisting limit cycle attractors, then a separate phase variable needs to be defined for each attractor.

10.1.2 Isochrons

The phase of oscillation can also be introduced outside the limit cycle. Consider, for example, point y_0 in Fig.10.2 (top). Since the trajectory $y(t)$ is not on a limit cycle, it is not periodic. However, it approaches the cycle as $t \to +\infty$. Hence, there is some point x_0 on the limit cycle, not necessarily the closest to y_0, such that

$$y(t) \to x(t) \quad \text{as} \quad t \to +\infty \,. \tag{10.2}$$

Now take the phase of the nonperiodic solution $y(t)$ to be the phase of its periodic proxy $x(t)$.

Alternatively, we can consider a point on the limit cycle x_0 and find all the other points y_0 that satisfy (10.2). The set of all such points is called *the stable manifold* of x_0. Since any solution starting on the stable manifold has an asymptotic behavior indistinguishable from that of $x(t)$, its phase is the same as that of $x(t)$. For this reason, the manifold represents solutions having equal phases, and it is often referred to as being the *isochron* of x_0 (*iso*, equal; *chronos*, time, in Greek), a notion going back to Bernoulli and Leibniz.

Every point on the plane in Fig.10.2, except the unstable equilibrium, gives rise to a trajectory that approaches the limit cycle. Therefore, every point has some phase. Let $\vartheta(x)$ denote the phase of the point x. Then, isochrons are level contours of the function $\vartheta(x)$, since the function is constant on each isochron.

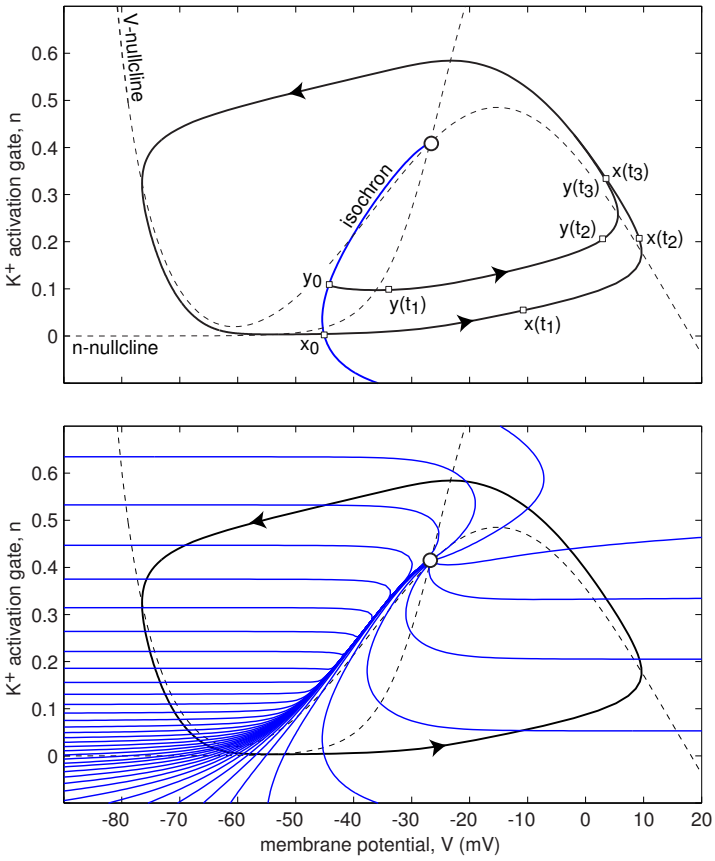

Figure 10.2: Top. An isochron, or a stable manifold, of a point x_0 on the limit cycle attractor is the set of all initial conditions y_0 such that $y(t) \to x(t)$ as $t \to +\infty$. Bottom. Isochrons of the limit cycle attractor in Fig.10.1 corresponding to 40 evenly distributed phases $nT/40$, $n = 1, \ldots, 40$.

The entire plane is foliated by isochrons. We depict only 40 representative ones in Fig.10.2. In this chapter we consider neighborhoods of exponentially stable limit cycles, where the foliation is continuous and invariant (Guckenheimer 1975):

- *Continuity.* The function $\vartheta(x)$ is continuous so that nearby points have nearby phases.
- *Invariance.* If $\vartheta(x(0)) = \vartheta(y(0))$, then $\vartheta(x(t)) = \vartheta(y(t))$ for all t. Isochrons are mapped to isochrons by the flow of the vector field.

Fig.10.3 shows the geometry of isochrons of various oscillators. The Andronov-Hopf oscillator in the figure is often called a radial isochron clock for the obvious reason. It is simple enough to be solved explicitly (see exercise 1). In general, finding isochrons is a daunting mathematical task. In exercise 3 we present a MATLAB program that finds isochrons numerically.

10.1.3 PRC

Consider a periodically spiking neuron (10.1) receiving a single brief pulse of current that increases the membrane potential by $A = 1$ mV, as in Fig.10.4 (left). Such a perturbation may not elicit an immediate spike, but it can change the timing, that is,

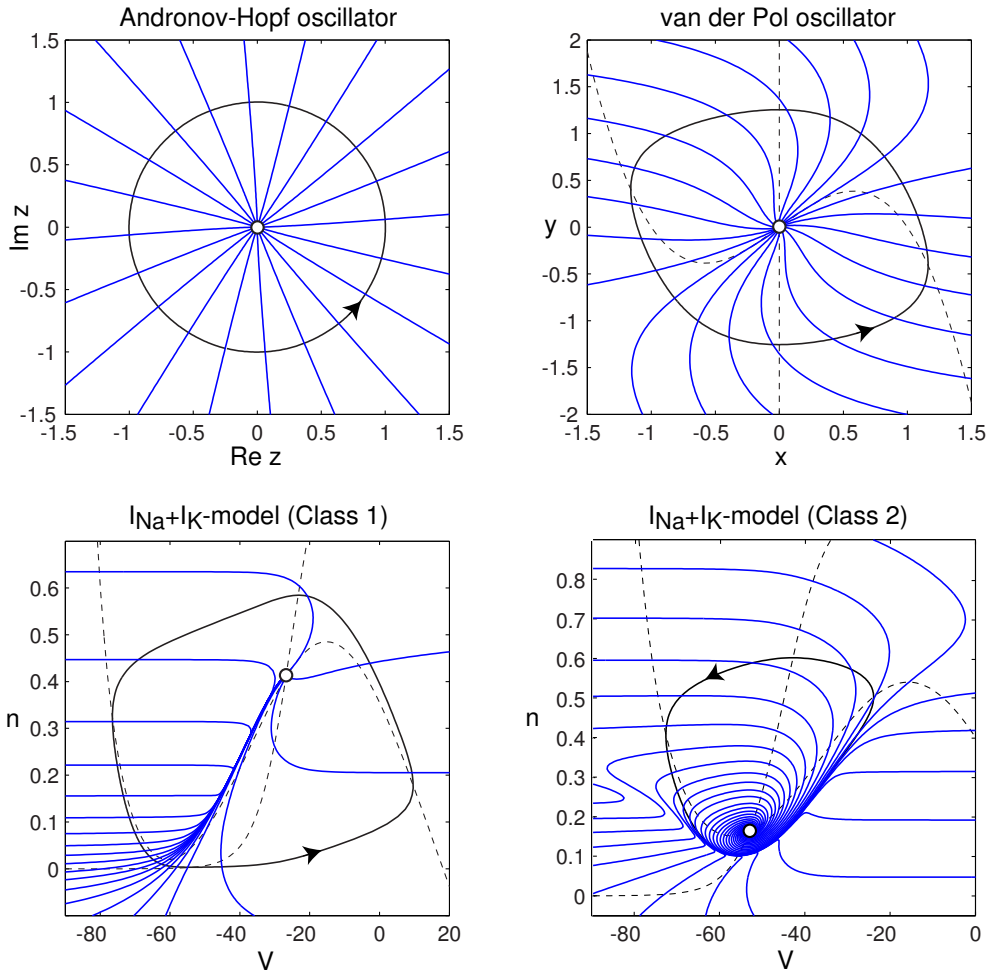

Figure 10.3: Isochrons of various oscillators. Andronov-Hopf oscillator: $\dot{z} = (1+\mathrm{i})z - z|z|^2$, $z \in \mathbb{C}$. van der Pol oscillator: $\dot{x} = x - x^3 - y$, $\dot{y} = x$. The $I_{\mathrm{Na}} + I_{\mathrm{K}}$-model with parameters as in Fig.4.1a and $I = 10$ (Class 1) and $I = 35$ (Class 2). Only isochrons corresponding to phases $nT/20$, $n = 1, \ldots, 20$, are shown.

the phase, of the following spikes. For example, the perturbed trajectory (solid line in Fig.10.4, left) fires earlier than the free-running unperturbed trajectory (dashed line). That is, right after the perturbation, the phase, ϑ_{new}, is greater than the old phase, ϑ. The magnitude of the phase shift of the spike train depends on the exact timing of the stimulus relative to the phase of oscillation ϑ. Stimulating the neuron at different phases, we can measure the *phase response curve* (also called phase-resetting curve PRC, or spike time response curve STRC)

$$\mathrm{PRC}\,(\vartheta) = \{\vartheta_{\mathrm{new}} - \vartheta\} \qquad (\text{shift} = \text{new phase} - \text{old phase})\ ,$$

depicted in Fig.10.4, right. Positive (negative) values of the function correspond to phase advances (delays) in the sense that they advance (delay) the timing of the next spike.

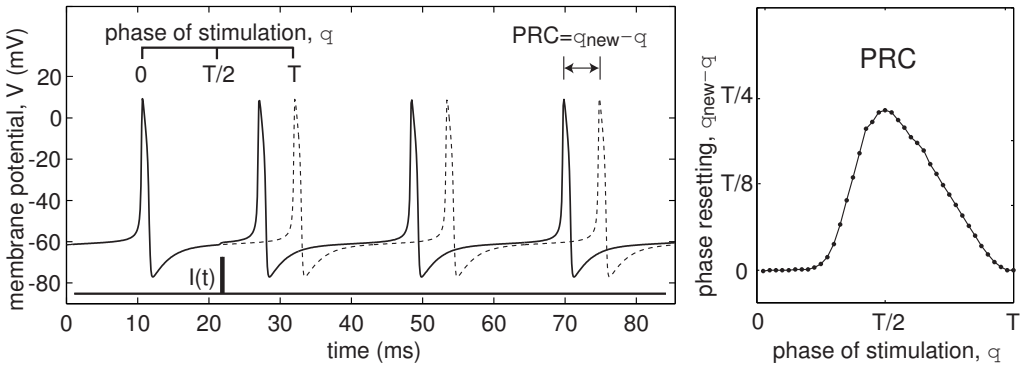

Figure 10.4: Phase response of the $I_{\rm Na}+I_{\rm K}$-model with parameters as in Fig.4.1a and $I=4.7$. The dashed voltage trace is the free-running trajectory.

In contrast to the common folklore, the function PRC (ϑ) can be measured for an arbitrary stimulus, not necessarily weak or brief. The only caveat is that to measure the new phase of oscillation perturbed by a stimulus, we must wait long enough for transients to subside. This becomes a limiting factor when PRCs are used to study synchronization of oscillators to periodic pulses, as we do in section 10.1.5.

There is a simple geometrical relationship between the structure of isochrons of an oscillator and its PRC, illustrated in Fig.10.5 (see also exercise 6). Let us stimulate the oscillator at phase ϑ with a pulse, which moves the trajectory from point x lying on the intersection of isochron ϑ and the limit cycle attractor to a point y lying on some isochron $\vartheta_{\rm new}$. From the definition of PRC, it follows that $\vartheta_{\rm new}=\vartheta+$PRC (ϑ).

In general, one uses simulations to determine PRCs, as we do in Fig.10.4. Using

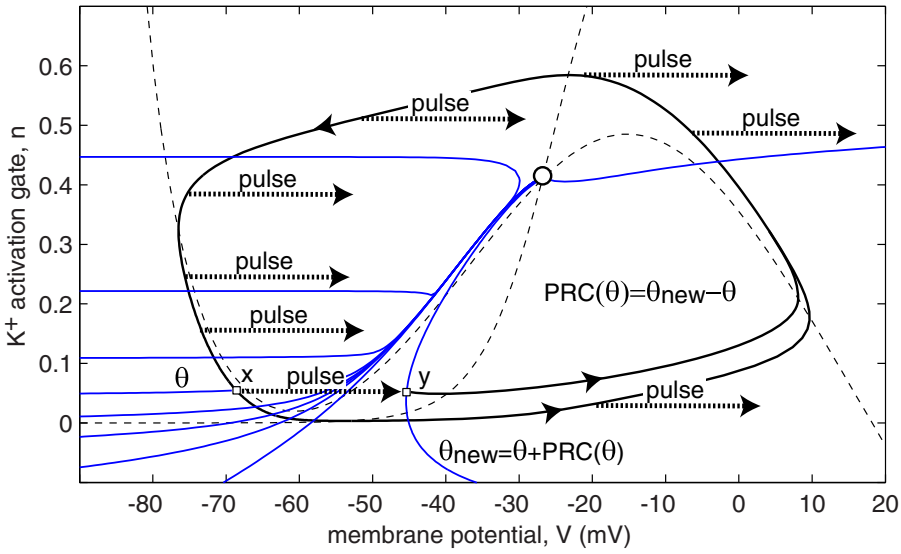

Figure 10.5: The geometrical relationship between isochrons and the phase response curve (PRC) of the $I_{\rm Na}+I_{\rm K}$-oscillator in Fig.10.1.

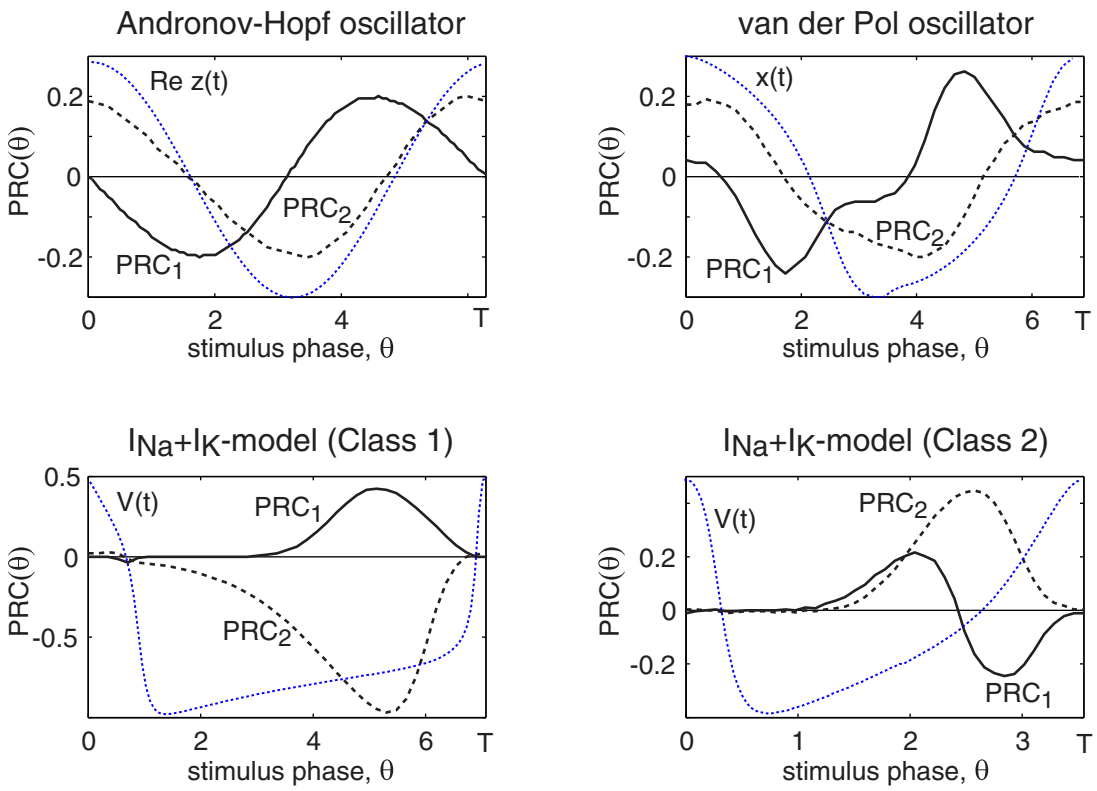

Figure 10.6: Examples of phase response curves (PRC) of the oscillators in Fig.10.3. $\mathrm{PRC}_1(\vartheta)$: Horizontal pulses (along the first variable) with amplitudes $0.2, 0.2, 2, 0.2$ for Andnronov-Hopf, van der Pol, Class 1 and Class 2 oscillators, respectively. $\mathrm{PRC}_2(\vartheta)$: Vertical pulses (along the second variable) with amplitudes $0.2, 0.2, 0.02, 0.002$, respectively. An example of oscillation is plotted as a dotted curve in each subplot (not to scale).

the MATLAB program presented in exercise 5, we can determine PRCs of all four oscillators in Fig.10.3 and plot them in Fig.10.6. It is a good exercise to explain the shape of each PRC in the figure, or at least its sign, using the geometry of isochrons of corresponding oscillators. In section 10.2.4 we discuss pitfalls of using the straightforward method in Fig.10.4 to measure PRCs in biological neurons, and we present a better technique.

Note that the PRC of the $I_{\mathrm{Na}} + I_{\mathrm{K}}$-model in Fig.10.6 is mainly positive in the Class 1 regime, that is, when the oscillations appear via saddle-node on invariant circle bifurcation, but changes sign in the Class 2 regime, corresponding in this case to the supercritical Andronov-Hopf bifurcation. In section 10.4 we find PRCs analytically in the case of weak coupling, and show that the PRC of a Class 1 oscillator has the shape $\sin^2 \vartheta$ (period $T = \pi$) or $1 - \cos \vartheta$ (period $T = 2\pi$), whereas that of a Class 2 oscillator has the shape $\sin \vartheta$ (period $T = 2\pi$). We show in section 10.1.7 how the synchronization properties of an oscillator depend on the shape of its PRC.

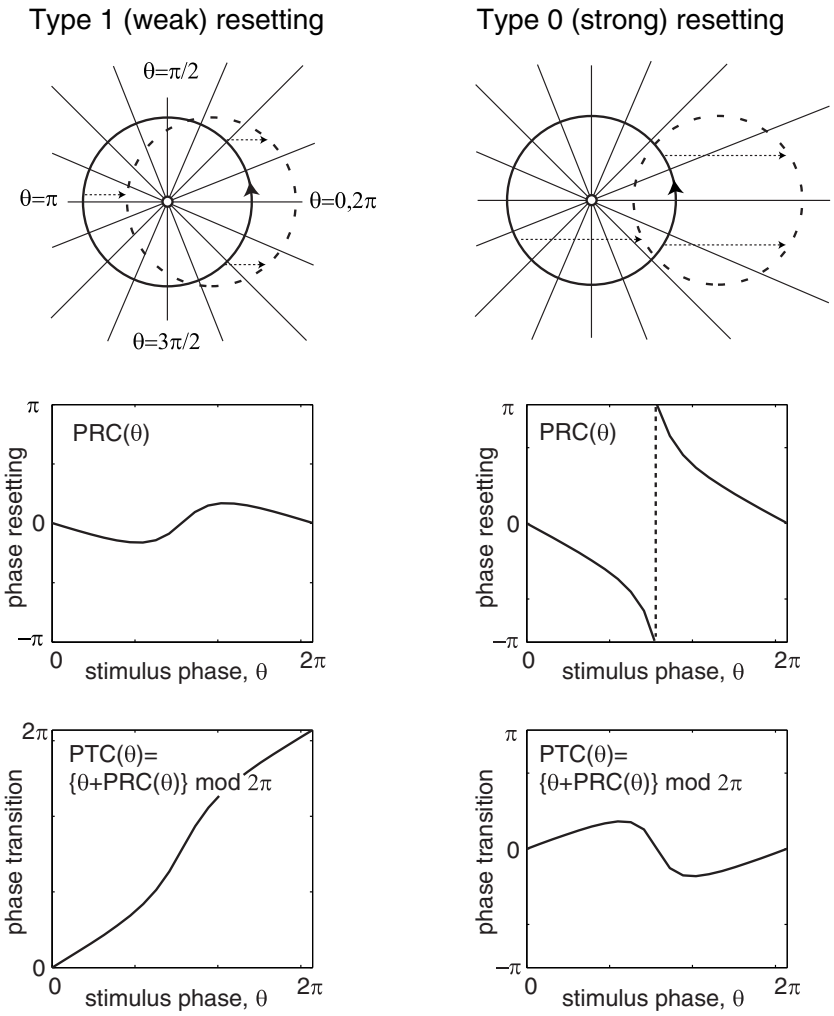

Figure 10.7: Types of phase-resetting of the Andronov-Hopf oscillator in Fig.10.3.

10.1.4 Type 0 and Type 1 Phase Response

Instead of phase-resetting curves, many researchers in the field of circadian rhythms consider *phase transition curves* (Winfree 1980)

$$\vartheta_{\text{new}} = \text{PTC}\,(\vartheta_{\text{old}}).$$

Since

$$\text{PTC}\,(\vartheta) = \{\vartheta + \text{PRC}\,(\vartheta)\} \bmod T,$$

the two approaches are equivalent. PRCs are convenient when the phase shifts are small, so that they can be magnified and seen clearly. PTCs are convenient when the phase shifts are large and comparable with the period of oscillation. We present PTCs in this section solely for the sake of review, and we use PRCs throughout the rest of the chapter.

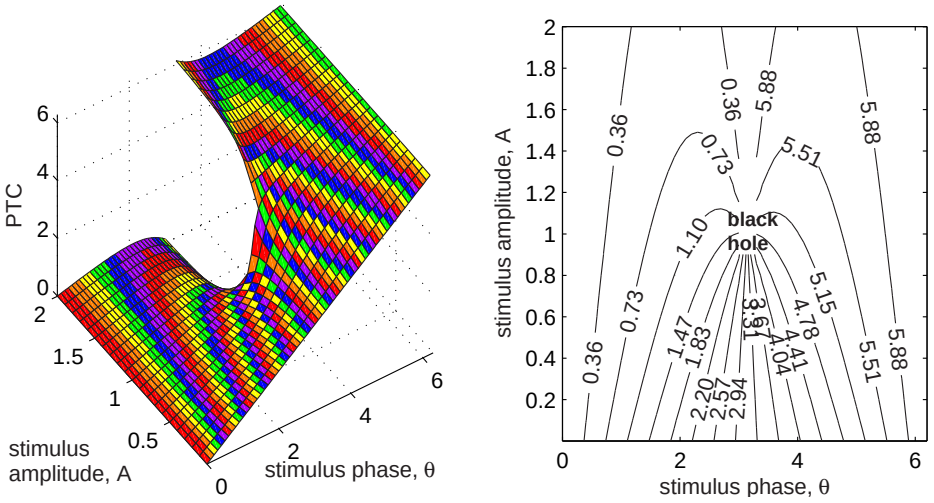

Figure 10.8: Time crystal (left) and its contour plot (right). Shown is the PTC (ϑ, A) of the Andronov-Hopf oscillator (see exercise 4).

In Fig.10.7 (top) we depict phase portraits of the Andronov-Hopf oscillator having radial isochrons and receiving pulses of magnitude $A = 0.5$ (left) and $A = 1.5$ (right). Note the drastic difference between the corresponding PRCs or PTCs. Winfree (1980) distinguishes two cases:

- *Type 1 (weak) resetting* results in continuous PRCs and PTCs with mean slope 1.

- *Type 0 (strong) resetting* results in discontinuous PRCs and PTCs with mean slope 0.

(Do not confuse these classes with Class 1, 2, or 3 excitability.) The discontinuity of the Type 0 PRC in Fig.10.7 is a topological property that cannot be removed by reallocating the initial point x_0 that corresponds to zero phase. As an exercise, prove that the discontinuity stems from the fact that the shifted image of the limit cycle (dashed circle) goes beyond the central equilibrium at which the phase is not defined.

If we vary not only the phase ϑ of the applied stimulus, but also its amplitude A, then we obtain parameterized PRC and PTC. In Fig.10.8 we plot PTC (ϑ, A) of the Andronov-Hopf oscillator (the corresponding PRC is derived in exercise 4). The surface is called *time crystal* and it can take quite amazing shapes (Winfree 1980). The contour plot of PTC (ϑ, A) in the figure contains the singularity point (black hole) that corresponds to the phaseless equilibrium of the Andronov-Hopf oscillator. Stimulation at phase $\vartheta = \pi$ with magnitude $A = 1$ pushes the trajectory into the equilibrium and stalls the oscillation.

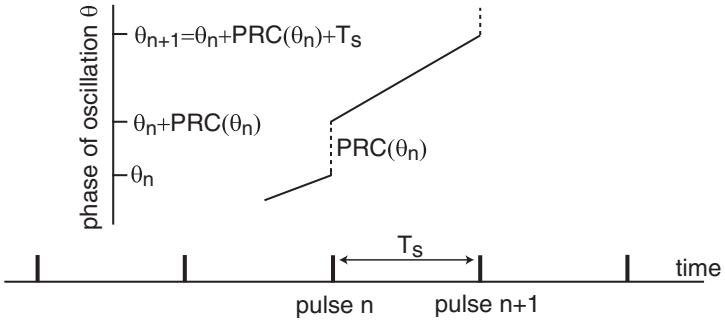

Figure 10.9: Calculation of the Poincare phase map.

10.1.5 Poincare Phase Map

The phase-resetting curve (PRC) describes the response of an oscillator to a single pulse, but it can also be used to study its response to a periodic pulse train using the following "stroboscopic" approach. Let ϑ_n denote the phase of oscillation at the time the nth input pulse arrives. Such a pulse resets the phase by $\mathrm{PRC}\,(\vartheta_n)$, so that the new phase right after the pulse is ϑ_n+$\mathrm{PRC}\,(\vartheta_n)$ (see Fig.10.9). Let T_s denote the period of pulsed stimulation. Then the phase of oscillation before the next, $(n+1)$th, pulse is ϑ_n+$\mathrm{PRC}\,(\vartheta_n) + T_\mathrm{s}$. Thus, we have a stroboscopic mapping of a circle to itself,

$$\vartheta_{n+1} = (\vartheta_n + \mathrm{PRC}\,(\vartheta_n) + T_\mathrm{s}) \mod T, \tag{10.3}$$

called the *Poincare phase map* (two pulse-coupled oscillators are considered in exercise 11). Knowing the initial phase of oscillation ϑ_1 at the first pulse, we can determine ϑ_2, then ϑ_3, and so on. The sequence $\{\vartheta_n\}$ with $n = 1, 2, \ldots$, is called the *orbit* of the map, and it is quite easy to find numerically.

Let us illustrate this concept using the $I_\mathrm{Na} + I_\mathrm{K}$-oscillator with PRC shown in Fig.10.4. Its free-running period is $T \approx 21.37$ ms, and the period of stimulation in Fig.10.10a is $T_\mathrm{s} = 18.37$, which results in the Poincare phase map depicted in Fig.10.10d. The cobweb in the figure is the orbit going from ϑ_1 to ϑ_2 to ϑ_3, and so on. Note that the phase ϑ_3 cannot be measured directly from the voltage trace in Fig.10.10a because pulse 2 changes the phase, so it is not the time since the last spike when pulse 3 arrives. The Poincare phase map (10.3) takes into account such multiple pulses. The orbit approaches a point (called a fixed point; see below) that corresponds to a synchronized or phase-locked state.

A word of caution is in order. Recall that PRCs are measured on the limit cycle attractor. However, each pulse displaces the trajectory away from the attractor, as in Fig.10.5. To use the PRC formalism to describe the effect of the next pulse, the oscillator must be given enough time to relax back to the limit cycle attractor. Thus, if the period of stimulation T_s is too small, or the attraction to the limit cycle is too slow, or the stimulus amplitude is too large, the Poincare phase map may be not an appropriate tool to describe the phase dynamics.

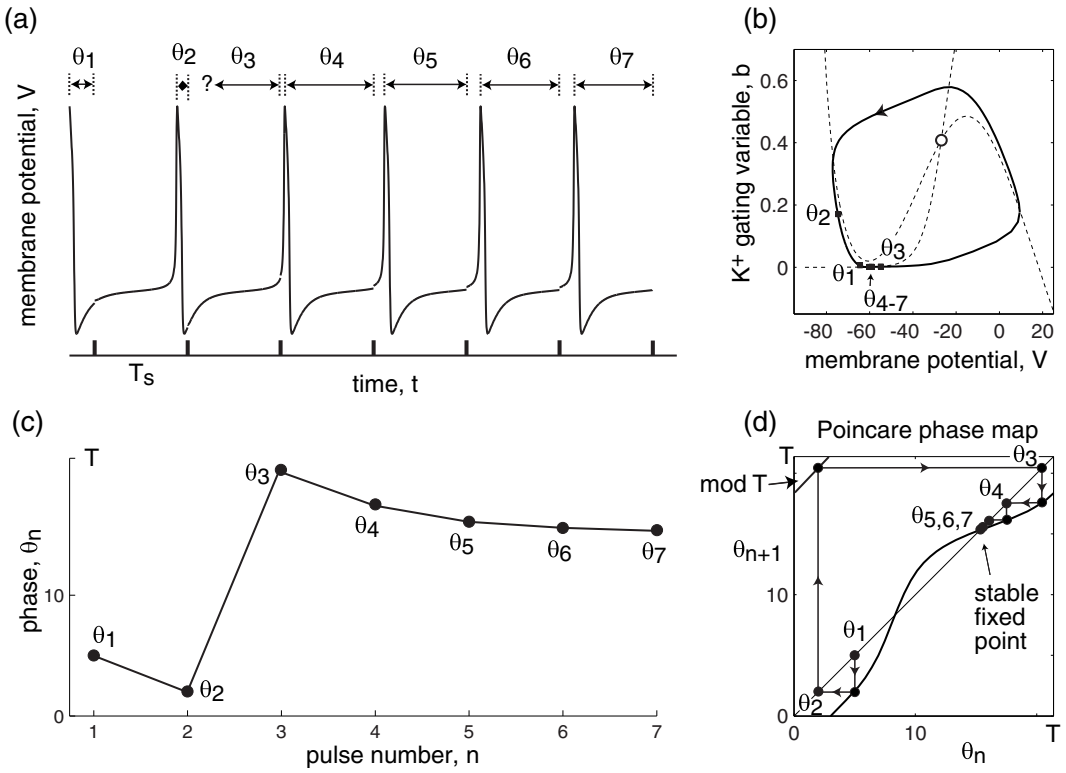

Figure 10.10: Description of synchronization of $I_{\rm Na} + I_{\rm K}$-oscillator in Fig.10.4, using Poincare phase map.

10.1.6 Fixed points

To understand the structure of orbits of the Poincare phase map (10.3), or any other map

$$\vartheta_{n+1} = f(\vartheta_n) \ , \tag{10.4}$$

we need to find its fixed points

$$\vartheta = f(\vartheta) \qquad (\vartheta \text{ is a fixed point}),$$

which are analogues of equilibria of continuous dynamical systems. Geometrically, a fixed point is the intersection of the graph of $f(\vartheta)$ with the diagonal line $\vartheta_{n+1} = \vartheta_n$ (see Fig.10.10d or Fig.10.11). At such a point, the orbit $\vartheta_{n+1} = f(\vartheta_n) = \vartheta_n$ is fixed. A fixed point ϑ is *asymptotically stable* if it attracts all nearby orbits, i.e., if ϑ_1 is in a sufficiently small neighborhood of ϑ, then $\vartheta_n \to \vartheta$ as $n \to \infty$, as in Fig.10.11, left. The fixed point is *unstable* if any small neighborhood of the point contains an orbit diverging from it, as in Fig.10.11 (right).

The stability of the fixed point is determined by the slope

$$m = f'(\vartheta)$$

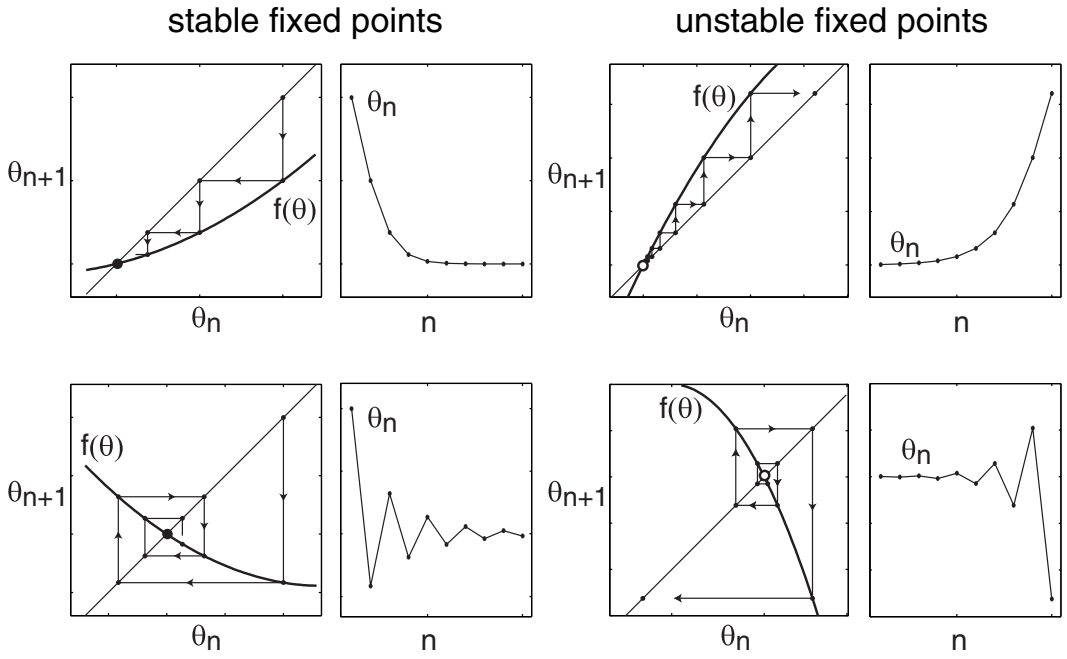

Figure 10.11: The stability of fixed points of the mapping (10.4) depends on the slope of the function f.

of the graph of f at the point, which is called the *Floquet multiplier* of the mapping. It plays the same role as the eigenvalue λ of an equilibrium of a continuous dynamical system. Mnemonically, the relationship between them is $\mu = e^{\lambda}$, to which the fixed point is stable when $|m| < 1$ ($\lambda < 0$) and unstable when $|m| > 1$ ($\lambda > 0$). Fixed points bifurcate when $|m| = 1$ (λ is zero or purely imaginary). They lose stability via flip bifurcation (a discrete analogue of Andronov-Hopf bifurcation) when $m = -1$ and disappear via fold bifurcation (a discrete analogue of saddle-node bifurcation) when $m = 1$. The former plays an important role in the period-doubling phenomenon illustrated in Fig.10.14 (bottom trace). The latter plays an important role in the cycle-slipping phenomenon illustrated in Fig.10.16.

10.1.7 Synchronization

We say that two periodic pulse trains are synchronous when the pulses occur at the same time or with a constant phase shift, as in Fig.10.12a. Each subplot in the figure contains an input pulse train (bottom) and an output spike train (top), assuming that spikes are fired at zero crossings of the phase variable, as in Fig.10.1. Such a synchronized state corresponds to a stable fixed point of the Poincare phase map (10.3). The in-phase, anti-phase, or out-of-phase synchronization corresponds to the phase shift $\vartheta = 0$, $\vartheta = T/2$, or some other value, respectively. Many scientists refer to the in-phase synchronization simply as "synchronization", and use the adjectives anti-phase and out-of-phase to denote the other types of synchronization.

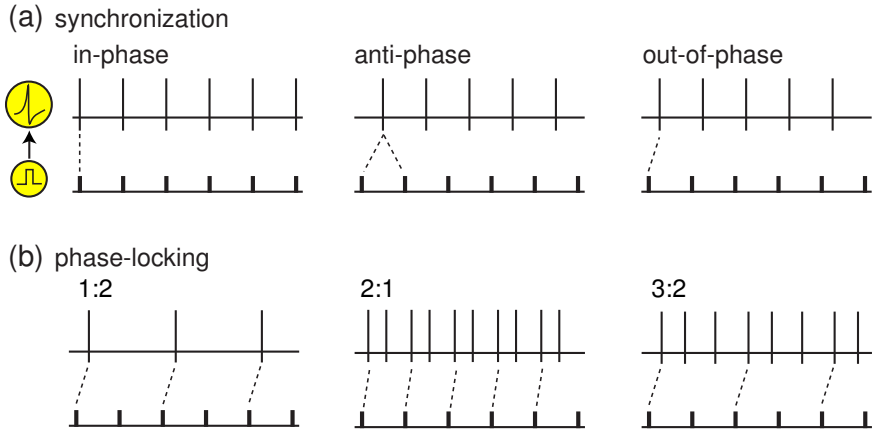

Figure 10.12: Examples of fundamental types of synchronization of spiking activity to periodic pulsed inputs (synchronization is 1:1 phase-locking).

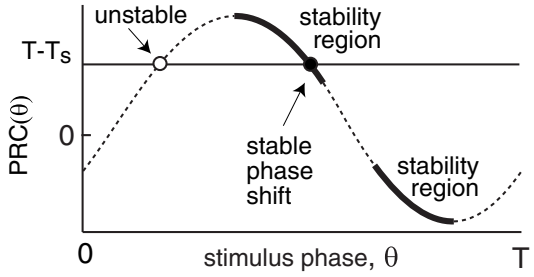

Figure 10.13: Fixed points of the Poincare phase map (10.3).

When the period of stimulation, $T_{\rm s}$, is near the free-running period of tonic spiking, T, the fixed point of (10.3) satisfies

$$\mathrm{PRC}\,(\vartheta) = T - T_{\rm s}\ ,$$

that is, it is the intersection of the PRC and the horizontal line, as in Fig.10.13. Thus, synchronization occurs with a phase shift ϑ that compensates for the input period mismatch $T - T_{\rm s}$. The maxima and the minima of the PRC determine the oscillator's tolerance of the mismatch. As an exercise, check that stable fixed points lie on the side of the graph with the slope

$$-2 < \mathrm{PRC}'(\vartheta) < 0 \qquad \text{(stability region)}$$

marked by the bold curves in Fig.10.13.

Now consider the Class 1 and Class 2 $I_{\rm Na} + I_{\rm K}$-oscillators shown in Fig.10.6. The PRC in the Class 1 regime is mostly positive, implying that such an oscillator can easily synchronize with faster inputs ($T - T_{\rm s} > 0$) but cannot synchronize with slower inputs. Indeed, the oscillator can advance its phase to catch up with faster pulse trains, but it cannot delay the phase to wait for the slower input. Synchronization with the input having $T_{\rm s} \approx T$ is only marginal. In contrast, the Class 2 $I_{\rm Na} + I_{\rm K}$-oscillator does not have this problem because its PRC has well-defined positive and negative regions.

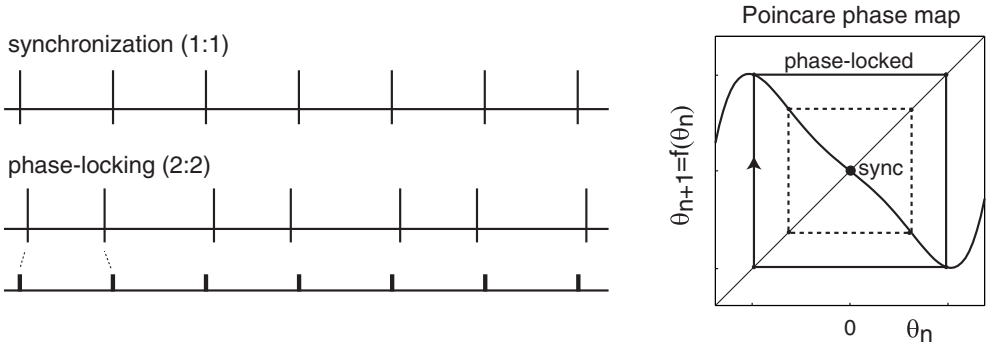

Figure 10.14: Coexistence of synchronized and phase-locked solutions corresponds to coexistence of a stable fixed point and a stable periodic orbit of the Poincare phase map.

10.1.8 Phase-Locking

The phenomenon of *p*:*q*-*phase-locking* occurs when the oscillator fires p spikes for every q input pulses, such as the 3:2-phase-locking in Fig.10.12b or the 2:2 phase-locking in Fig.10.14, which typically occurs when $pT \approx qT_{\rm s}$. The integers p and q need not be relatively prime in the case of pulsed-coupled oscillators. Synchronization, that is, 1:1 phase-locking, as well as p:1 phase-locking corresponds to a fixed point of the Poincare phase map (10.3) with p fired spikes per single input pulse. Indeed, the map tells the phase of the oscillator at each pulse, but not the number of oscillations between the pulses.

Each p:q-locked solution corresponds to a stable periodic orbit of the Poincare phase map with the period q (so that $\vartheta_n = \vartheta_{n+q}$ for any n). Such orbits in maps (10.4) correspond to stable equilibria in the iterates $\vartheta_{k+1} = f^q(\vartheta_k)$, where $f^q = f \circ f \circ \cdots \circ f$ is the composition of f with itself q times. Geometrically, studying such maps is like considering every qth input pulse in Fig.10.12b and ignoring all the intermediate pulses.

Since maps can have coexistence of stable fixed points and periodic orbits, various synchronized and phase-locking states can coexist in response to the same input pulse train, as in Fig.10.14. The oscillator converges to one of the states, depending on the initial phase of oscillation, but can be switched between states by a transient input.

10.1.9 Arnold Tongues

To synchronize an oscillator, the input pulse train must have a period $T_{\rm s}$ sufficiently near the oscillator's free-running period T so that the graph of the PRC and the horizontal line in Fig.10.13 intersect. The amplitude of the function $|\mathrm{PRC}\,(\vartheta, A)|$ decreases as the strength of the pulse A decreases, because weaker pulses produce weaker phase shifts. Hence the region of existence of a synchronized state shrinks as $A \to 0$, and it looks like a horn or a tongue on the $(T_{\rm s}, A)$-plane depicted in Fig.10.15, called *Arnold tongue*. Each p:q-phase-locked state has its own region of existence (p:q-tongue in the

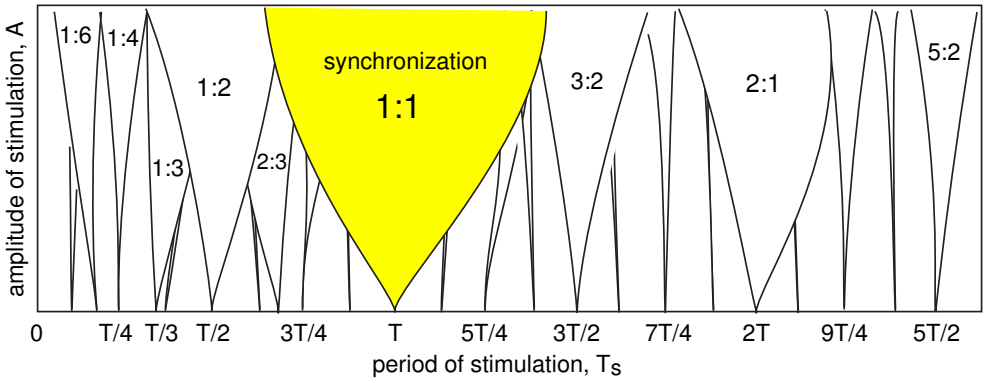

Figure 10.15: Arnold tongues are regions of existence of various phase-locked states on the "period-strength" plane.

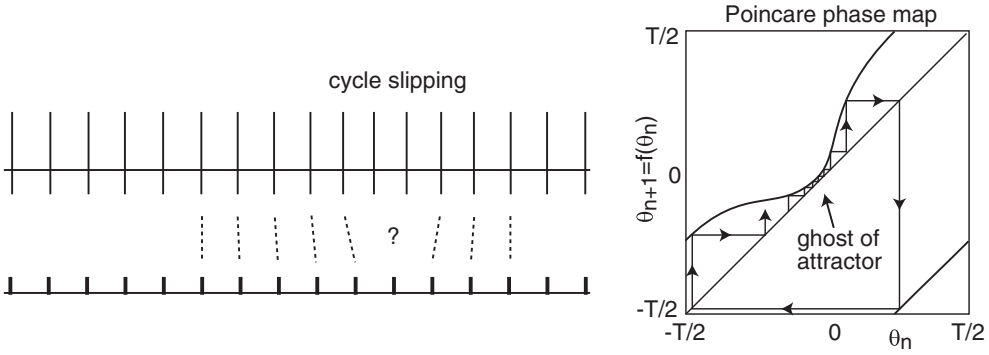

Figure 10.16: Cycle slipping phenomenon at the edge of the Arnold tongue corresponding to a synchronized state.

figure), which also shrinks to a point pT/q on the T_s-axis. The larger the order of locking, $p+q$, the narrower the tongue and the more difficult it is to observe such a phase-locked state numerically, let alone experimentally.

The tongues can overlap, leading to the coexistence of phase-locked states, as in Fig.10.14. If A is sufficiently large, the Poincare phase map (10.3) becomes noninvertible, that is, it has a region of negative slope, and there is a possibility of chaotic dynamics (Glass and Mackey 1988).

In Fig.10.16 we illustrate the *cycle slipping* phenomenon that occurs when the input period T_s drifts away from the 1:1 Arnold tongue. The fixed point of the Poincare phase map corresponding to the synchronized state undergoes a fold bifurcation and disappears. In a way similar to the case of saddle-node on invariant circle bifurcation, the fold fixed point becomes a ghost attractor that traps orbits and keeps them near the synchronized state for a long period of time. Eventually the orbit escapes, the synchronized state is briefly lost, and then the orbit returns to the ghost attractor to be trapped again. Such an intermittently synchronized orbit typically corresponds to a p:q-phase-locked state with a high order of locking $p+q$.